Sains Malaysiana 46(11)(2017): 2049-2059
http://dx.doi.org/10.17576/jsm-2017-4611-05

Environmental Geological Features of the Red Clay Surrounding Rock Deformation under the Influence of Rock-Fracture Water

(Ciri Geologi Persekitaran Lempung Merah Mengelilingi Canggaan Batuan di bawah Pengaruh Retakan- Batuan Air)

Jiading Wang*, Tianfeng Gu, Jianbin Wang, Yuanjun Xu, Peng Chen & Muhammad Aqeel Ashraf

ABSTRACT

The development degree of fissure water in underground rock is a great trouble to the construction of railway tunnel, which will cause a series of environmental geological problems. Take the surrounding rock-section of the typical red clay in Lvliang-Mt. railway tunnel below the underground water level as an example, several aspects about the red clay surrounding rock will be researched, including pore water pressure, volume moisture content, stress of surrounding rock, vault subsidence and horizontal convergence through the field monitoring. Taking into account the importance of railway tunnel engineering, the large shear test of red clay was carried out at the construction site specially and the reliable situ *shear strength parameters of surrounding rock will be obtained. These investigations and field tests helped to do a series of work: Three dimensional finite element numerical model of railway tunnel will be established, the deformation law of the red clay surrounding rock will be investigated, respectively, for the water-stress coupling effect and without considering it, the variation of the pore water pressure during excavation, the influence degree about the displacement field and stress field of water-stress coupling on red clay-rock will be discussed and the mechanism of the surrounding rock deformation will be submitted. Finally, the paper puts forward the feasible drainage scheme of the surrounding rock and the tunnel cathode. The geological environment safety of tunnel construction is effectively protected.*

Keywords: Deformation features; environmental geological problems; railway tunnel; red clay surrounding rock; rock-fracture water

ABSTRAK

Tahap perkembangan rekahan air di dalam batuan bawah tanah merupakan masalah besar untuk pembinaan landasan terowong yang akan menyebabkan satu siri masalah geologi alam sekitar. Sebagai contoh, lihat pada bahagian batuan sekeliling tanah liat tipikal di terowong landasan Lvliang-Mt. di bawah paras air bawah tanah, beberapa aspek tentang tanah liat merah di sekeliling batuan akan diteliti, termasuk tekanan air pori, isi padu kandungan lembapan, tekanan batuan keliling, penurunan vault dan konvergensi mendatar melalui pemantauan lapangan. Dengan mengambil kira kepentingan kejuruteraan terowong keretapi, ujian ricih besar tanah liat merah dilakukan di tapak pembinaan khasnya dan parameter kekuatan ricih situ *yang boleh dipercayai di sekitar batuan akan diperoleh. Kajian dan ujian lapangan ini membantu melakukan satu siri kerja: Tiga elemen dimensi terhingga unsur model terowong kereta api akan ditubuhkan, undang-undang canggaan tanah liat merah di sekeliling batu akan dikaji untuk tekanan gandingan tekanan air dan tanpa mempertimbangkannya, variasi tekanan air liang semasa penggalian, darjah pengaruh tentang medan anjakan dan tegasan gandingan tekanan air pada tanah liat merah akan dibincangkan dan mekanisme canggaan batuan di sekeliling akan dikemukakan. Kesimpulannya, kertas ini mengemukakan skim saliran yang sesuai di sekitar batu dan katod terowong. Keselamatan geologi alam sekitar untuk pembinaan terowong dilindungi dengan berkesan.*

Kata kunci: Air batu-pecah; ciri ubah bentuk; landasan terowong; masalah geologi alam sekitar; tanah liat merah di sekeliling batu

Introduction

Shanxi South Central Railway is the key project of Chinese 11th five-year plan and it is also the first ten-thousand ton class heavy load railway. Along the railway, there are many tunnels and foundation built in a special soil stratum which named Hipparion red soil. In Lvliang-Mt. area (Duowen & Derbyshire 1991), the Hipparion red soil is the most typical. The mechanical property of Hipparion red soil will decrease when the moisture content increase, which would induce accident. For instance, the surrounding rock of Lvliang-Mt. railway tunnel is affected by groundwater, which changed the moisture content of Hipparion red soil and induced the crack of initial liner, displacement of side wall and collapse of vault. This environmental geological property of Hipparion red soil affects the construction and designs a lot (Feng et al. 2013).

At present, many researchers have studied the stability of tunnel engineering and accumulated valuable experience. But, the studies on Hipparion red soil are concentrated on the Magnetic fabric (Gong et al. 2015), chronology (Flynn et al. 2011) and grain size characteristics (Liu et al. 2007). There is rare study on environmental geology features of Hipparion red soil (Chu et al. 2005; Hao & E-Chuan 2015; Hashimoto et al. 2005; Kataoka et al. 2015). Zeng et al. (1991) analyze the erosion rule of Hipparion red soil in northwestern area of Shanxi province and pointed out that the erosion intensity is quite related to gradient, moisture content of soil, freeze-thaw action and wind. Wang et al. (2012) summarized the progress of microstructure test and creep test on Hipparion red soil and also analyzed the mechanism of landslides controlled by Hipparion red soil. Evans et al. (1991) and Shi et al. (2013) analyzed the engineering geology features of Hipparion red soil in Bao-ji city and pointed out that under the effect of groundwater action the shear strength of Hipparion red soil will decrease.

To sum up, some researchers have conducted studies of engineering geology features Hipparion red soil, but rare research related to the Hipparion red soil as surrounding rock. Our research group has conducted some studies on it, such as: grain size, palaeo geomagnetic dating, physical and mechanical property and microstructure scanning. Based on these studies, the tunnel surrounding rock stability has been studied. But, that study is just 2-D, which did not take 3-D stability into consideration. Therefore, in this research, the Hipparion red soil surrounding rock under groundwater has been taken as research object and the moisture content, pore pressure, surrounding rock stress, vault and side wall deformation were monitored and analyzed. Based on that, the shear strength parameters of surrounding rock was got from *in-situ* large scale shear test, then the 3-D finite element numerical model was built, which took the water-force coupling action into consideration, meanwhile the other model which did not take the water-force coupling action into consideration was also be built (Tayeb et al. 2016). Then, through the calculation and analysis, the pore water pressure change discipline and the effect degree of water-force coupling action on surrounding rock stress and displacement field were pointed out. The deformation and failure mechanism of surrounding rock was also discussed.

The aims of this research were: To predict process of tunnel surrounding rock stress deformation and failure; and to further speculate that the influence of emergence, runoff and gush of underground fissure water on rock deformation and tunnel construction safety. In addition, it can also fully predict groundwater decline, groundwater captured around soil area, destruction of capillary water migration pathway and effect of forest grassland ecological environment because of underground fissure water change.

Materials and Methods

Environmental geological condition of tunnel surrounding rock deformation

The railway tunnel in western Shanxi Province was designed according to double-track railway standard. The whole length is 12.807 km, the length of the tunnel that the Hipparion red soil as surrounding rock is 6 km and about 4.44 km of that is located under the groundwater table. The thickness of soil above the tunnel is in the range of 5 to 184 m and the thickness of Hipparion red soil is in the range of 0 to 85 m, which is mainly distributed in entrance and exit of the tunnel. Figure 1 shows the classic section of tunnel.

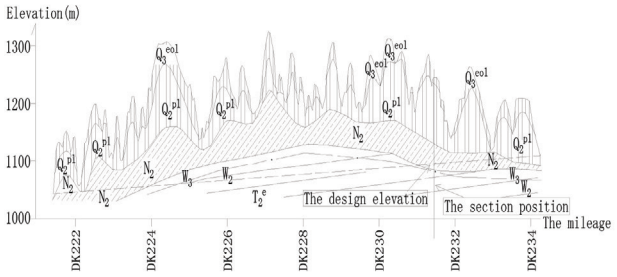

FIGURE 1. Railway Tunnel section in western Shanxi Province

The study area is located at Xi country where the terrain undulation is big, the altitude difference is in the range of 40 to 265 m. The *in-situ* features of Hipparion red soil are as follows: Hard plastic, not uniform, several layers of calcareous concretion, well developed joint fissures and most of them are slightly open. The tunnel face is moist and the ground water seep from the fissures (Hennie et al. 2017). There is ponding in the inverted arch, which is caused by the lager area seepage form side walls of the new excavated tunnel without second layer liner. At this section, the thickness of covering soil is 175.3 m, in which the new loess is 31.9 m, the old loess is 88.1 m and the Hipparion red soil is 55.3 m. The substratum is intense weathering sandstone and moderately weathered sand-mudstone.

Field monitoring

Monitoring content and method

As is known to all, it is dangerous to get the deformation monitoring of tunnel face. However, in order to get firsthand information of tunnel face, we risked injury by caved rock at any moment to embedded sensors and carried out field monitoring. The main content of field monitoring included volumetric water content, pore water pressure, surrounding rock stress, the vault subsidence and horizontal convergence.

VOLUMETRIC WATER CONTENT

In this, the FDS-100 soil moisture sensor was used to monitor the volumetric water content, which has the probe-centered measurement range which ranged from 0 to 85% and was surrounded by a 7 cm tall and 7 cm in diameter cylinder.

PORE WATER PRESSURE

The BX Pore water pressure sensor was used in this test which was also output the voltage signal and the Measuring range was 100kPa.

SURROUNDING ROCK STRESS

In this, the BX resistance-type soil pressure cell with the range of 1.0 MP was used to monitor the surrounding rock stress.

THE VAULT SUBSIDENCE AND HORIZONTAL CONVERGENCE

The measurement of vault subsidence was accomplished by setting measuring point on the tunnel vault. After the initial supporting, we used pneumatic drill to drill and inbuilt pothook which should not exposure to much to avoid the damage by the machine. In this research, one measure point was laid in the central of the arch. Datum mark was kept away from the monitoring section and total station was used to measure. The difference between the initial reading and the later is vault subsidence (Hennie et al. 2017; Rahim et al. 2017; Tayeb et al. 2016).

The layouts of measuring points of horizontal convergence were symmetrical. After the initial supporting, we used pneumatic drill to drill and inbuilt pothook, then used plain concrete mortar to tamping, after the solidification, monitoring conducted. In this research, two measuring line were laid, the measuring points of horizontal convergence and vault subsidence were located on the same layer. We used HS-67 convergence meter and monitored regularly. The difference between the initial reading and the later is horizontal convergence.

In this experiment, 14 sensors were used which included 8 soil pressure sensors, 4 pore water pressure sensors, 2 soil water pressure sensors, 1 point of the vault subsidence and two measuring line of horizontal convergence, as shown in Figure 2.

Analysis of field monitoring results

The field monitoring began in cross hatching excavation and last 70 days which obtained a large number of measured data.

THE CHARACTERISTIC OF WATER CONTENT CHANGES

Figure 3 shows the change of water content with the change of time. The difference of water content at different position is remarkable with 16.18% at top step and 17.46% at lower step. With the continuing of time, the water content witnessed a linear growth. The basic stability of the water content was appeared two months later which is approximate saturation condition. With the vertical comparison, it is obvious that the water content of top step was greater the water content of lower step from beginning to end. There are two reasons that account for this phenomenon. Firstly, the side wall and baseboard of surrounding rock suffered larger crushing stress than other parts, as a result, there are a lot of fracture which can be seen in field. With high seepage and pore water pressure, the crack reinforces the infiltration capacity of rock. Secondly, after the second liner timbering, as the resist of flashing underground water transfer download along the flashing, which resulted the underground water converged at lower step and increase the water content of lower step.

THE CHARACTERISTIC OF PORE WATER PRESSURE

Figure 4 shows the relation between pore water pressure and time. The change of pore water pressure of the arch crown, haunch and side wall shown the increase of linear growth. Earlier and middle stage of monitoring, the red clay was unsaturated. Relevantly the curve shown that the pore water pressure of surrounding rock was less than zero and had the increase tendency with the continuing increasing of water content. When the monitoring continue about 2 months, the water content of surrounding rocks is nearly saturation condition and the pore water pressure changed from minus to plus zone and continuing increase until the end of monitoring.

With the supporting structure of up, middle and below step and waterproofing measures completed progressively, as the inverted arch was located in the bottom of tunnel, the groundwater was gathered to the inverted arch along the flashing (Rahim et al. 2017). Two hours after excavation the water head appeared and the highest reached 1 m.

Before the construction of inverted arch, the red soil of the bottom of tunnel was under saturation condition, therefore, pore water pressure was always greater than zero and the speed of pore water pressure increasing was range from quick to slow, at last the surrounding rock reached saturation condition until the monitoring and the pore water pressure was approximately 19.9 kPa.

THE CHARACTERISTIC OF SURROUNDING ROCK STRESS

Figure 5 shows the relation between surrounding rock stress and time. With the time change, the surrounding rock stress increased and tended to stabilization. It may be divided into three stages: Growth period, conditioning period and stable period. In the initial stage of tunnel excavation (0~20 days) the surrounding rock stress increased sharply, reached the 80%~95% of maximum stress. Especially the left side which increased fastest and the maximum was approximately 700 kPa. The reason for this phenomenon was that the surrounding rock was destabilized by the tunnel excavation, as a result the stress of deep surrounding rock transferred and freed to free face which formed the area of stress concentration. In the stress adjustment period (20~60 days), the tendency of surrounding rock stress change was the slowly increasing or increased to maximum then decreased little by little

This is because the finish of the preliminary bracing of top step and the successive excavation of middle and below step resulted to the surrounding rock stress got adjusted with the second and third redistribution. The excavation of middle and below step resulted the below surrounding rock unloading.as the supporting structure the stress of the upside surrounding rock transfer to middle and below step, which has proved by the figure. In this stage, surrounding rock stress fluctuated and had slightly decline as a whole. After the adjustment, the surrounding rock stress presented a stabilization stage (from the 60 day to the end of monitoring).

Overall the stress of rocks is large. The rock stress of top left corner is approximately 900 kPa and stability of 650 kPa in the end, meanwhile the rock stress of top right corner is less than 100 kPa. This is because in three steps and seven stages excavation method, the rock of top left corner was firstly excavated with no preliminary bracing, as a result, the free face appeared at the top left corner which the release rate of original crustal stress was higher than other positions. Relatively, when the work of top right corner began, most of the crustal stress of the surrounding rocks had released, what is more, the supporting structure was more complete, therefore, the rock stress of the top right corner was lower.

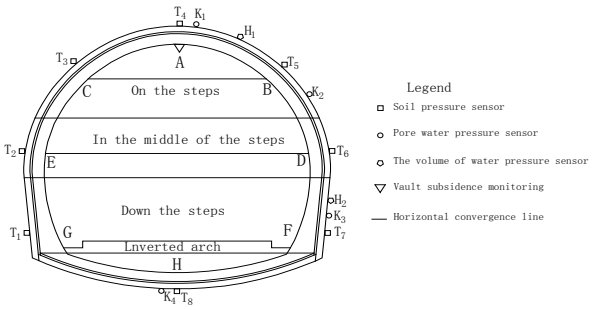

FIGURE 2. Distribution of monitoring geophone for tunnel surrounding rock deformation

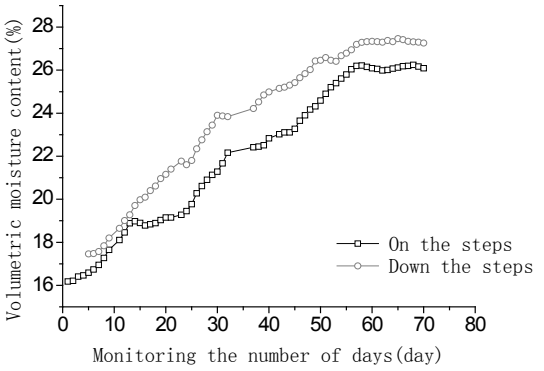

FIGURE 3. The relationship between volumetric water content and time

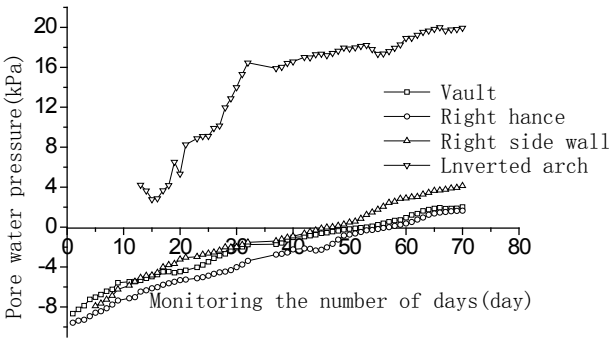

FIGURE 4. The relationship between pore water pressure and time

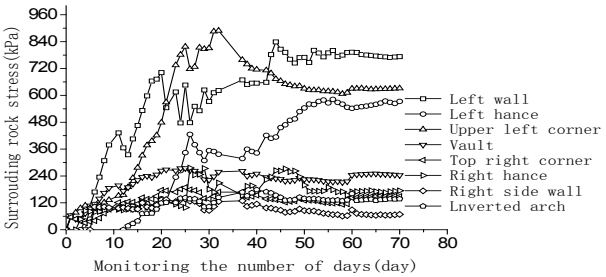

FIGURE 5. The relationship between surrounding rock stress and time

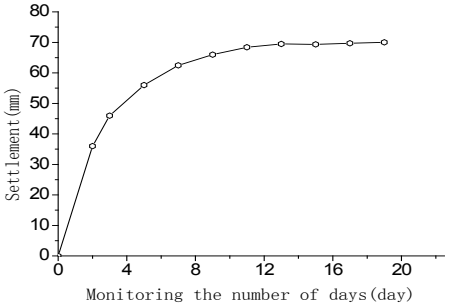

FIGURE 6. Vault subsidence temporal curves

THE CHANGE RULE OF VAULT CROWN SETTLEMENT

As shown in Figures 6-7, in the first 2 days, the speed of vault crown settlement was fastest, and then the speed decreased gradually and turns to zero. The stress state of surrounding rocks changed from three-dimensional to bi-directional. The imbalance of stress resulted in the surrounding rocks to produce displacement to free face which was the sudden submerges of vault. Until the 17 days, the accumulation of vault crown settlement was 65.78 mm which accounted to 95%.

According to the rule of the change of displacement rate in the railway tunnel construction specifications and the design specifications, when the speed of displacement 0.19 mm/day <0.2 mm/day, the surrounding rock tend to stable. After the monitoring, all the arch subsidence was up to 69.25 mm.

THE CHANGE RULE OF HORIZONTAL CONVERGENCE

As shown in Figures 7-8, the change rule of horizontal convergence is similar as the tendency of crown settlement, but there are differences in the speed of displacement. The speed of level convergence which the maximum is 11.22 mm/day was lower than the speed of vault crown which the maximum is 18 mm/day. The change of horizontal convergence can be divided into three stages in all.

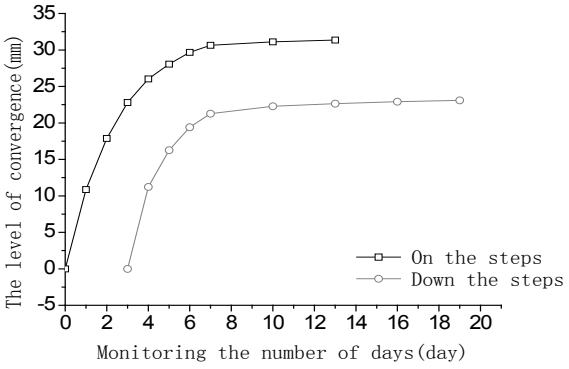

FIGURE 7. The level of convergence temporal curve

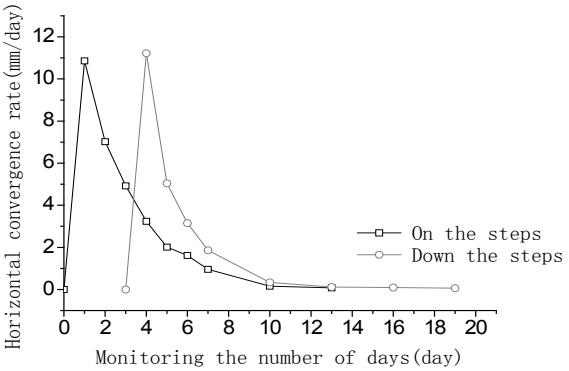

FIGURE 8. Temporal curve level convergence rate

NUMERICAL MODELING

According to the result of *in-situ* monitoring, the surrounding rock deformation feature of hipparion red soil is affected by groundwater seepage prominently. In order to research the surrounding wall deformation feature and mechanical behavior of hipparion red soil under the environment of groundwater seepage, the profile of monitoring was treated as object of study, and then a large-scale shear test on the soil was conducted in the refuge hole. The shear strength parameter was entered into 3D model of numerical analysis. Then the deformation of surrounding rock was calculated considering and does not take into account the force-water coupling.

IN-SITU LARGE-SCALE SHEAR TEST

The method of this test is double acting jack, one of them applies the vertical load and the other applies the horizontal load. The schematic diagram of the test equipment is as shown in Figure 9.

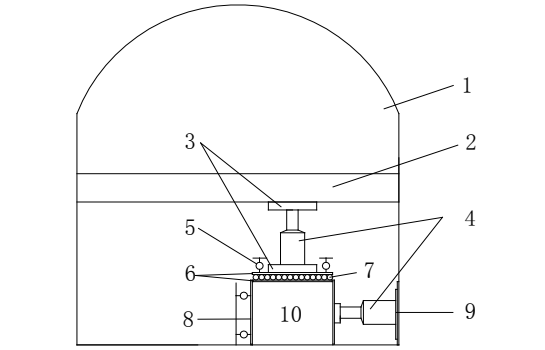

FIGURE 9. *In situ* shear plane sketch

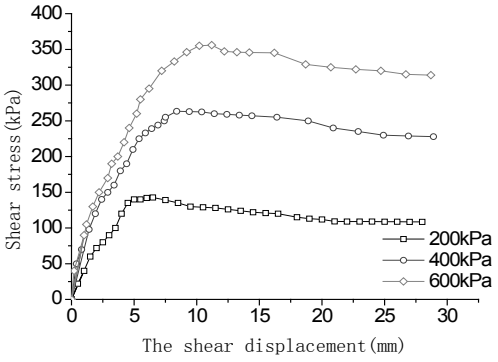

FIGURE 10. Shear stress-displacement curve

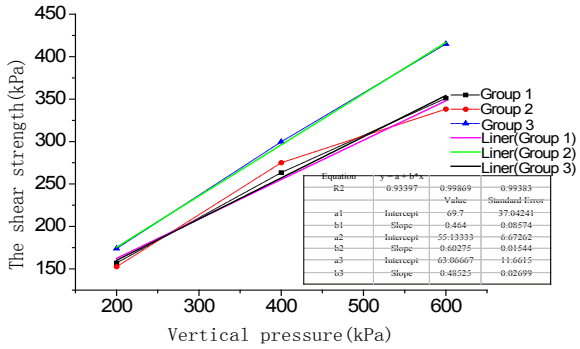

FIGURE 11. Hipparion red soil shear curve and its fitting

The natural moisture content is 18.5%, the plastic limit is 19.0% and the liquid limit is 30.5%. Considering there is groundwater seepage in the surrounding wall, the test sample was considered as saturated soil. The specimen size is 500 × 500 × 400 mm (length × width × height).

The shear area is 500 × 400 mm and the estimated value of vertical load is 200, 400 and 600 kPa, according to the estimated value of c, φ from the Mohr-Coulomb formula to estimate the shear load. Then, vertical and horizontal load will be divided into 10 parts and it will be applied on the sample step by step. First, apply the vertical load, next, the vertical load level can be applied when the deformation is less than 0.05 mm per 5 min, and under the last level of vertical load, if the deformation is less than 0.05 mm in two straight for 15 min, the vertical deformation can be counted as steady state. After that, the shear load can be applied on the sample. The shear failure criteria are as follow: When the shear stress peak value appeared, the test should stop and if the peak value does not appear, when shear deformation increase sharply or when the shear deformation is larger than the one-tenth length of sample the test should stop.

Figure 10 shows the shear stress-displacement curve of hipparion red soil. The shape of curve shows the trend of hardening, with the increase of shear deformation, the shear stress increase sharply at first and then change to be steady and there is no obvious peak value of shear stress. This indicates that the structural strength of hipparion red soil is high, which cause the small residual deformation and the major stress strength are shared by structural strength. The diagenesis degree of hipparion red soil is high and it contains lot of calcareous concretion which play an anchored structure role and it make hipparion red soil got some rock mechanical features.

TABLE 1. Large *in situ* shear strength parameter statistics

No.	1	2	3
C(kPa)	63.1	63.1	68.6
φ(°)	25.9	26.1	29.7

Figure 11 shows the Hipparion red soil shear curve and its fitting and base which we summarize in Table 1.

From the comparison, we can see that there is a big difference between each soil sample, and it may be related to the moisture content. The shear strength of Hipparion red soil is high when it is under natural conditions. But it should be noticed that there are a lot of micro fissures in the soil, under the long term erosion by the ground water, the soluble salt will be dissolved, which will decline the combination strength between soil particles. On the other hand, the ground water also can lead the expansion of micro fissures and make them connect with each other finally. Under the aforementioned action, the shear strength will be declined. Therefore, we choose the parameters as follows: C=60.0 kPa, φ=27.7°.

MODEL BUILDING

In order to simplify the model and decrease the influence of boundary conditions, the range of the model is as follow: On horizontal direction, along with the tunnel axis, the model will be extended to 80 m; the lower boundary of the model is 65 m below the bottom of tunnel; the upper boundary of the model is extended to ground surface and the cover layer is 175 m. The stratum from upper to lower will be as follows: New loess, old loess, hipparion red soil, intense weathered sand shale and medium weathered san shale, as shown in Figure 12.

The stratum is simulated by 8 note 6 surface grid and the yield criterion is Mohr-Coulomb criterion and the constitutive model is elastic-plastic model. In the model, there are 116385 nodes and 97663 elements.

The displacement boundary of model is sated as follow: The normal constrains is all around, and the bottom of the model is fixed boundary.

Seepage boundary is proposed. Based on condition of groundwater depth and the worst condition of seepage boundary that survey's data showed, settled water head boundary is set to 55 m for left and right face, dank boundary is set on underside and anteroposterior faces. If initial supporting of tunnel does not produce water stop effect, water head of the lining face will be set to zero, that is to say, the lining face is seepage face. Before per excavation of tunnel, first we add seepage boundary and seepage face for seepage flow calculation, then proceed to calculation of excavation and supporting of tunnel.

Simulation of bolt adopts linear implantable truss element simulation. It realizes node automatic coupling, what is more, it is convenient and realistic.

We propose the steel fabric shotcrete and steel arch shelf as an equivalent body and adopting two-dimensional plate unit simulation. Shotcrete can be divided into soft sprayed and hard sprayed, these two phases are used for simulating process of initial supporting, initial supporting phase simulate early process of initial supporting and hard sprayed phase simulate later process of initial supporting.

Calculated parameters were chosen based on comprehensive analyzing, laboratory tests, codes of practice and engineering experience, soil layer and calculated parameters of supporting structure are shown in Table 2.

Analysis of Computing Result

Analysis of Pore Water Pressure

Figure 13 shows the change of pore water pressure before and after the construction. Before construction, the pore water pressure was equally distributed. The pore water pressure changed obviously with the tunnel excavation. There are funnel area around the lining surface. The hydraulic gradient was the maximum nearly the lining surface, which leaded to the bigger hydrodynamic pressure and a trend to instability of the surrounding rock of red clay.

Analysis of Seepage Analysis

Figure 14 shows the change of the velocity of groundwater flow. With the tunnel excavation, the ground water seepage from the far-field to tunnel and lead to change of pore water pressure. The velocity of groundwater flow in the horizontal orientation was mainly distributed in the connection of steps and the maximum velocity of groundwater flow was distributed in arch springing and the connection of inverted arch and down step (about 400 mm/day). The maximum of vertical velocity of groundwater flow was distributed the connection of inverted arch and down step (about 170 mm/day). It shows the arch springing and the connection of inverted arch and down step were catchment area, which was in accordance with the result of field research. Although the groundwater flow was slow, with the long time seepage the surrounding rock of tunnel arch springing was easily to cause seepage deformation and even buckling failure.

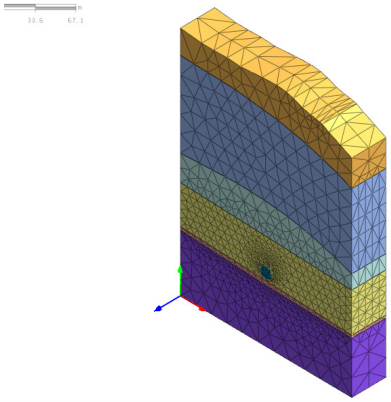

FIGURE 12. Three-dimensional calculation model

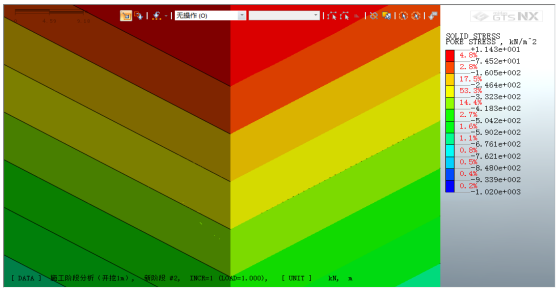

(a) Unexcavated

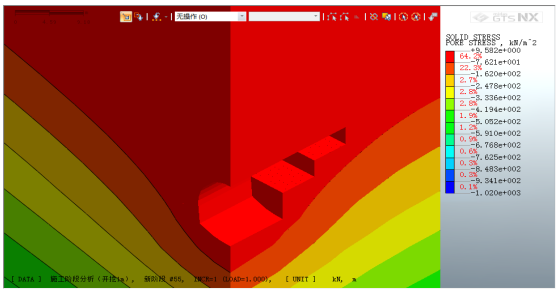

(b) Excavated 4m

FIGURE 13. Pore water pressure field change before and after the construction

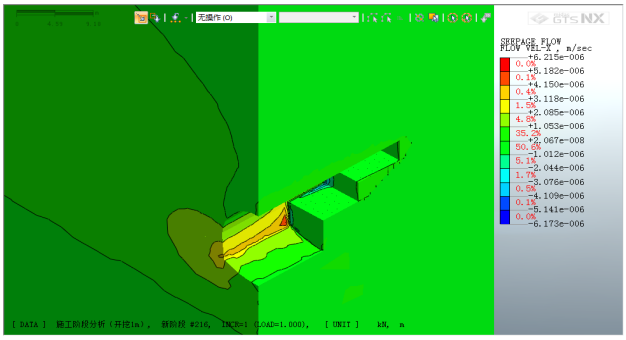

(a)excavated 4m horizontal flow field

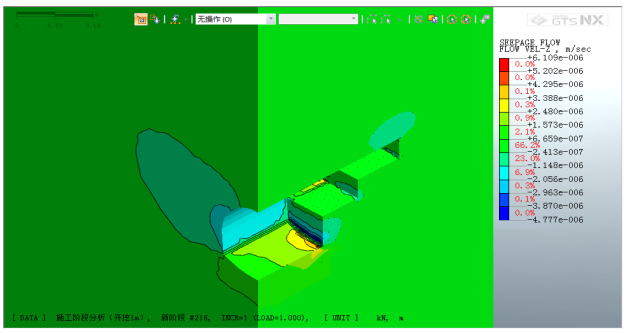

(b) excavated 4m vertical flow field

FIGURE 14. In the process of the construction velocity state nephogram

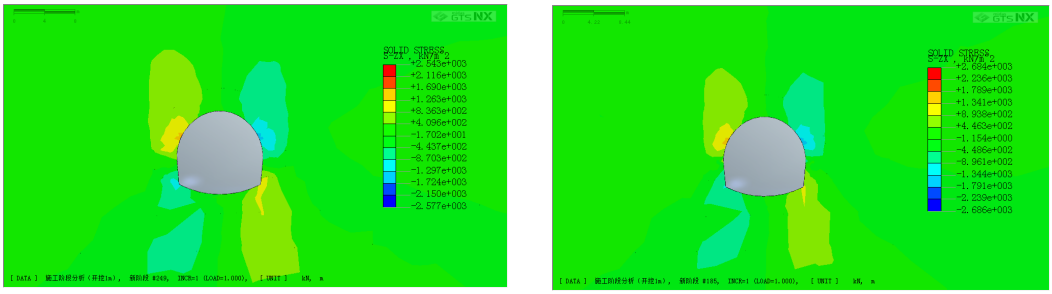

(a) consider Hydro-mechanical coupling (b) without consider Hydro-mechanical coupling

FIGURE 15. in the construction process of shear stress nephogram

ANALYSIS OF STRESS FIELD

Figure 15 shows the shear stress during construction. Considering the hydro-mechanical (HM) coupling, the shear stress of surrounding rocks were distributed around tunnel as 'X' and there were shear stress concentration in haunch and arch springing. Compared to no considering the hydro-mechanical (HM) coupling, the range of shear stress concentration was larger when considered the hydro-mechanical (HM) coupling. The concentrated shear stress was about 2577 kpa when considered the hydro-mechanical (HM) coupling. Contrary, the concentrated shear stress was about 2684 kpa. Although the shear stress was lower when considered the hydro-mechanical (HM) coupling, the groundwater flow had highly weaken the strength of surrounding rocks, which would easily result in shear failure in haunch and arch springing and was badly to the stabile of surrounding rock.

Figure 16 shows the maximum of shear strain during construction. The maximum shear strain was distributed symmetrically along the centre of tunnel. When considering the hydro-mechanical (HM) coupling, there were max shear strain in haunch, side wall and tunnel bottom which were within the scope of 1.5 m of surrounding rocks of tunnel surface. Relatively, when we do not considering the Hydro-mechanical (HM) coupling, there were max shear strain in haunch, side wall and tunnel bottom which were within the scope of 1 m of surrounding rocks of tunnel surface. It reflected that the seepage force strengthen the shear strain of surrounding rock, especially in the bottom of tunnel. With the construction of tunnel excavation, the seepage of groundwater would lead to the decrease of pore water pressure of surrounding rock and lead to the consolidation settlement of surrounding rock in the bottom of tunnel, then, strengthen the range of plastic zone of surrounding rock.

ANALYSIS OF SURROUNDING ROCK HORIZONTAL DISPLACEMENT

Figure 17 shows the distribution of horizontal displacement of surrounding rock during construction. The horizontal displacement were distributed symmetrically along the centre of tunnel, which main distributed in haunch and arch springing and manifest as the horizontal convergence of center and below surrounding rock. When considering the Hydro-horizontal mechanical (HM) coupling, the horizontal converged range was obvious increased and the max horizontal converged displacement was about 149 mm which increased by 7.1% compared to no considering the hydro-horizontal mechanical (HM) coupling which was 139 mm. This shows that the ground water flow had significantly influence on the horizontal displacement of surrounding rock.

Figure 18 shows the relation between horizontal displacement and the location of tunnel face. Considering groundwater flow, the difference of the horizontal displacement between the up and below side wall was obvious.

TABLE 2. Modle calculation parameters

Materials	γ/KN.m^{-3}	Es/MPa	λ	C/kPa	φ/(°)	k/m.d^{-1}
New loess	16.5	65	0.35	37	25.4	1.0
Old loess	17.9	90	0.35	48	26.8	0.5
Hipparion red	19.0	160	0.30	150	29.0	0.1
soil(upon water)	-	-	-	-	-	-
Hipparion red	19.8	130	0.33	64	27.7	0.2
soil(under water)	-	-	-	-	-	-
Strong	22.0	300	0.25	200	32.0	0.1
weathered mudstone	-	-	-	-	-	-
Medium	24.0	500	0.22	600	35.0	1.0E-05
weathered mudstone	-	-	-	-	-	-
Soft sprayed concrete	24.0	16241	0.2	-	-	-
Hard sprayed concrete	24.0	26241	0.2	-	-	-
anchor arm	78.5	210000	0.2	-	-	-

γ- Unit weight; Es- Elastic Modulus; λ- Poisson's ratio; C- Cohesive strength; φ-Internal friction angle; k- Permeability coefficient

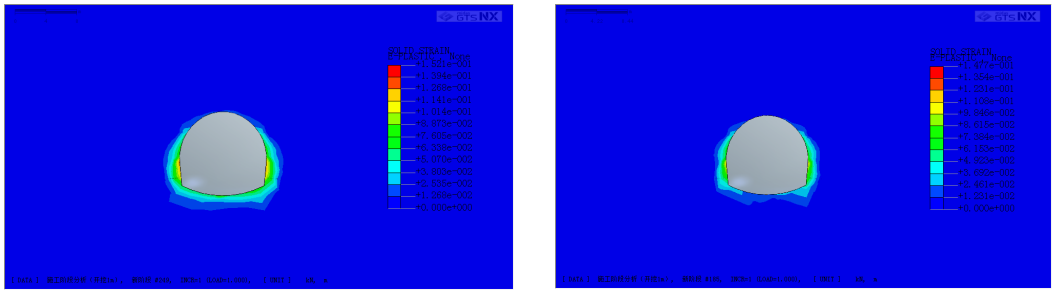

(a) consider Hydro-mechanical coupling (b) without consider Hydro-mechanical coupling

FIGURE 16. Construction in the process of maximum shear strain nephogram

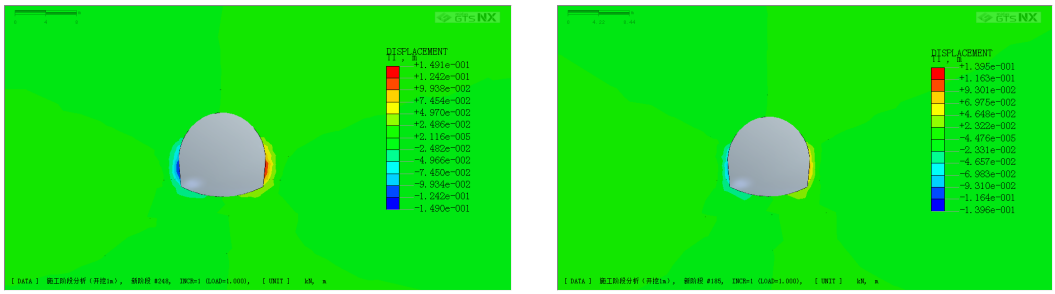

(a) consider Hydro-mechanical coupling (b)without consider Hydro-mechanical coupling

FIGURE 17. Horizontal displacement distribution nephogram in the course of construction

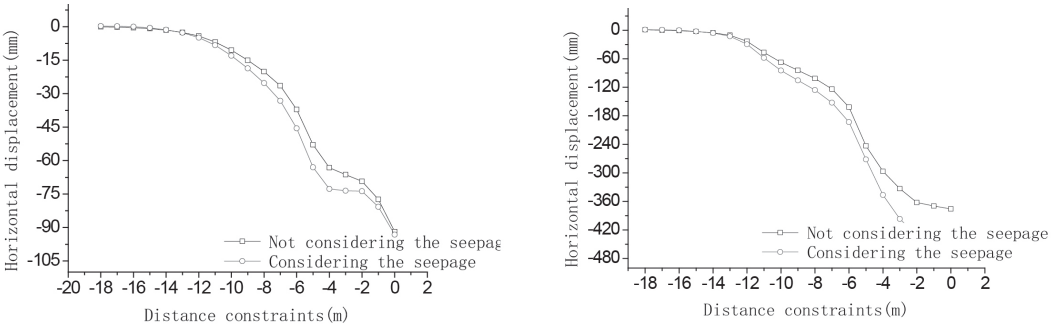

(a)upper side wall (b) lower side wall

FIGURE 18. The horizontal displacement of surrounding rock and constraints position relation curve

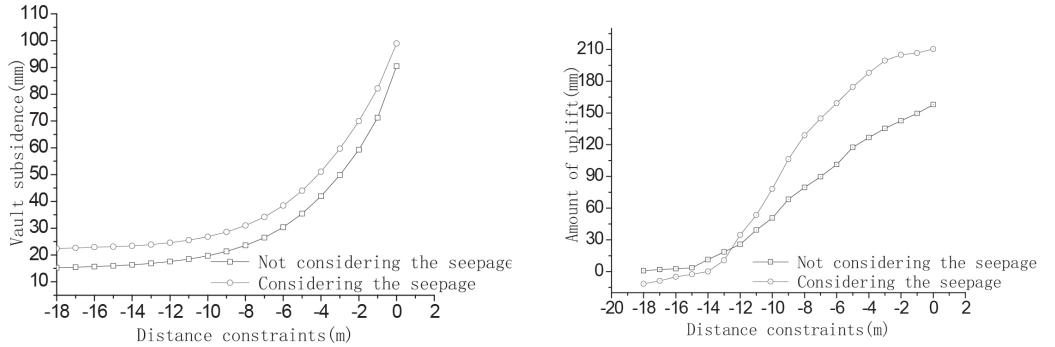

(a) Vault (b) Bottom

FIGURE 19. The vertical displacement of surrounding rock and constraints position relation curve

Figure 19 shows the distribution of vertical displacement of surrounding rock which was distributed symmetrically along the center of tunnel. The arch unloaded and subsided by gravity, which become the main subsided area. The floor heaved and become the main heave area. Compared to the max arch subside (158 mm) and floor uplift (119 mm) which no considering the hydro-horizontal mechanical (HM) coupling, the max arch subside (164 mm) and floor heave (120 mm) considering the hydro-horizontal mechanical (HM) coupling were increased relatively 5.0% and 0.8%. It reflected that the groundwater flow had a obvious and negative influence on the whole stabile of surrounding rock.

Discussion of surrounding rock deformation mechanism

Base on the summary of the field investigation, *in-situ* monitor and numerical simulation, the way of water-force coupling interaction is shown as Figure 20. Following the tunnel excavation, the equilibrium state of groundwater seepage would be broken; meanwhile the hydraulic free face will appear. Under the effect of excavation and surrounding rock support, the ground water will flow through vault and side wall and the water will gather at the bottom of tunnel. As a kind of special soil, Hipparion red soil contains a lot of micro fissures. Under the effect of excavate unloading, the surrounding rock stress will relaxation, which will make the micro fissures spread all over the surrounding rock. Then, under the effect of ground water seepage, the soluble salt will dissolved which will lead the broken of soil skeleton, and this process will aggravate the soil discontinuity. The soil discontinuity provide new path to groundwater and impact on the seepage filed.

As time goes by, the groundwater seepage field will come to the new balance, meanwhile the pressure of pore water will decrease to be steady, which will cause the increase of effective stress of surrounding rock and change the stress field. As aforementioned, the shear strength of Hipparion red soil is sensitive to moisture content,

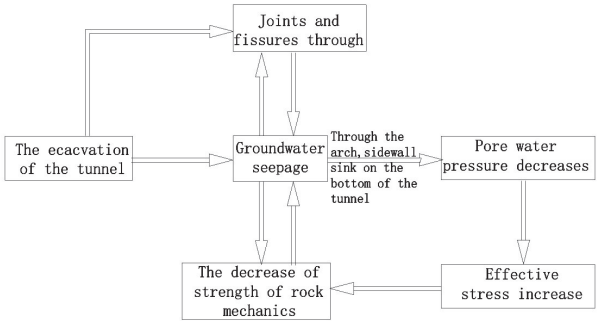

FIGURE 20. Water - force coupling field interaction way schemes

therefore, we can predict that when the moisture content changed to saturated state, the shear strength of surrounding rock will decrease sharply. Conversely, these 3 factors of high effective stress, low strength of surrounding rock and connected joint fissure impacted on the ground water seepage. Therefore, to protect the stability of surrounding rock, the water gathered at the bottom of tunnel should be drain away and the inverted arch should be built.

Conclusion

Based on the Shi-Lou tunnel project, through the method of *in-situ* monitoring, large scale shear test and numerical simulation, the deformation feature and the mechanism of surrounding rock under the phreatic line has been analyzed and discussed, the conclusions are as follows:

The *in-situ* monitoring shows that the deformation of vault is bigger than that of side wall, therefore, the support of vault should be enhanced. The stress level is high which can be divided into 3 phases: increase phase (before 20 days), adjustment phase (21~60 days) and stable phase (after 60 days). The moisture content of lower step is higher than higher step and become to saturated condition around 60 days and the pore water pressure changed form negative value to positive value.

The relationship between shear stress and shear displacement of Hipparion red soil shows harden trend. The structure strength is big, which is very sensitive to water action. On one hand, ground water action decrease the combination strength of soil skeleton, on the other, under the effect of excavation, the micro fissures become connection, which weaken the strength further.

The result of numerical simulation shows that the pore water pressure field changed a lot after tunnel excavation. This situation is caused by the change of ground water flow velocity, and the funnel-shaped zone of pore water pressure makes the increase of hydraulic gradient, which will lead the soil sustain more hydrodynamic pressure. Water-force coupling action impact on the surrounding rock shear stress, max-shear strain distribution and its value notably. Considering the effect of groundwater seepage and the water-force coupling action, the settlement of vault, displacement to side wall and uplift of tunnel floor will be bigger than without considering the effect.

Following the tunnel excavation, the hydraulic free face of groundwater will form near the tunnel lining. Under the effect of tunnel excavation and supporting, the groundwater will flow through the vault, the sidewall and will gather at bottom of tunnel finally and this progress will make the expansion of joint fissures, which will become the preferential passage of groundwater. Then, the pore pressure will be decrease, which will lead the increase of effective stress, therefore, when the moisture content becomes saturated, the shear strength will decrease sharply. Conversely, these 3 factors of high effective stress,

low strength of surrounding rock and connected joint fissure impacted on the ground water seepage. Therefore, to protect the stability of surrounding rock, the water gathered at the bottom of tunnel should be drain away and the inverted arch should be built.

This study can predict the tunnel surrounding rock stress deformation and failure process and further speculate that emergence, runoff and gush of underground fissure water has influence on rock deformation and tunnel construction safety. In addition, it can also fully predict groundwater decline, groundwater captured around soil area, destruction of capillary water migration pathway and effect of forest grassland ecological environment because of underground fissure water change.

ACKNOWLEDGEMENTS

The paper is mainly funded by the National Natural Science Foundation of China (41630639, 40972193) and State Key Laboratory of Continental Dynamics Foundation (2014). Hereon, we gave our deepest gratitude to them and those who assist in ensuring the completion of this paper.

REFERENCES

Chu, W.J., Xin, M.G. & Cai, Y.T. 2015. Analysis of deformation characteristics and support measures in upper tertiary clay tunnel. *Journal of Railway Engineering Society* 32(6): 40-44.

Duowen, M. & Derbyshire, E. 1991. The depositional environment of the late Pliocene "red clay", Jing-Le Basin, Shanxi Province, China. *Sedimentary Geology* 70(1): 33-40.

Evans, M.E., Wang, Y., Rutter, N. & Ding, Z.L. 1991. Preliminary magnetostratigraphy of the red clay underlying the loess sequence at Baoji, China. *Geophysical Research Letters* 18(8): 1409-1412.

Feng, J., Lu, J.F., Shi, Y.C. & Zhou, C.H. 2013. Mechanical response of surrounding rock of tunnels constructed with the TBM and drill-blasting method. *Natural Hazards* 66(2): 545-556.

Flynn, L.J. Deng, T., Wang, Y., Xie, G.P., Hou, S.K., Pang, L.B., Wang, T.M. & Mu, Y.Q. 2011. Observations on the *Hipparion* red clays of the Loess Plateau. *Vertebrata Palasiatica* 49(3): 275-284.

Gong, H.J., Zhang, R., Yue, L.P., Zhang, Y.X. & Li, J.X. 2015. Magnetic fabric from Red clay sedimentsin the Chinese Loess Plateau. *Scientific Reports* 5: 9706.

Hao, Z. & E-Chuan, Y. 2015. The surrounding rock deformation and failure mechanism of wudang group schists tunnel. *Electronic Journal of Geotechnical Engineering* 20(15): 6557-6576.

Hashimoto, Y., Nakaya, T. & Song, S.R. 2005. Distribution of deformation features and clay mineral characteristics around the Chelung-pu Fault, Taiwan. *Acta Mechanica Solida Sinica 18(1): 1-12*.

Hennie, F.W.S.E., Asis, J., Abdullah, M., Musta, B., Tahir, S., Pungut, H. & Husin, M.A.Y.M. 2017. Geochemical characterization of sediments around nukakatan valley, Tambunan, Sabah. *Geological Behavior* 1(1): 13-15.

Kataoka, M., Obara, Y. & Kuruppu, M. 2015. Estimation of fracture toughness of anisotropic rocks by semi-circular bend (SCB) tests under water vapor pressure. *Rock Mechanics and Rock Engineering* 48(4): 1353-1367.

Liu, J., Qiao, Y. & Guo, Z. 2007. The differences of grain size of quarts and bulk samples as an indicator of weathering intensity in the Aeolian deposits. *Quaternary Sciences* 2007(2): 270-276

Rahim, I.A., You, L.K. & Salleh, N.M. 2017. Kampung Mesilou landslide: The controlling factors. *Geological Behavior* 1(1): 19-21.

Shi, S.J., Qu, Y.X., Li, B. & Wu, S.R. 2013. Engineering geological properties of Neogene hard clays in Baoji City area, Shaanxi Province, and their effect on slope failure *Geological Bulletin of China* 32(12): 1918-1924 (In Chinese).

Wang, G.L., Zhang, M.S. & Wu, F.Q. 2012. Review on study of mechanism of loess landslides conteollled by hipparion red clay; *Proceedings of the 9th national conference on Engineering Geology. China's Shandong Qingdao.* pp. 170-174 (in Chinese).

Zeng, B.Q., Ma, W.Z. & Zhang, Z.G. 1991. Study on erosion of slumping in Sanzhima red clay area. *Bulletin of Soil Water Conservation* 7: 21-28.

Tayeb, M.A., Ismail, B.S., Mardiana, K.J. & Ta, G.C. 2016. Troubleshooting and maintenance of high-performance liquid chromatography during herbicide analysis: An overview. *Sains Malaysiana* 45(2): 237-245.

Jiading Wang*, Tianfeng Gu, Jianbin Wang, Yuanjun Xu & Peng Chen
State Key Laboratory of Continental Dynamics
Northwest University
Xi'an 710069
China

Muhammad Aqeel Ashraf
International Water, Air & Soil Conservation Society
59200 Kuala Lumpur, Federal Territory
Malaysia

*Corresponding author; email: wangjd@nwu.edu.cn

Received: 1 February 2017
Accepted: 4 June 2017